ELSEVIER

Catalysis Today 41 (1998) 111–128

CATALYSIS TODAY

Genesis, architecture and nature of sites of Co(Ni)–MoS_2 supported hydroprocessing catalysts

J. Grimblot*

Laboratoire de catalyse hétérogène et homogène, URA CNRS 402, Université des Sciences et Technologies de Lille, 59655 Villeneuve d'Ascq Cédex, France

Abstract

The present paper examines some features relevant to hydroprocessing reactions over MoS_2 supported catalysts promoted by Co or Ni. After the description of the main classes of reactions, catalyst genesis and activation (i.e. sulphidation) are extensively described and discussed. The final part deals with the identification of the catalyst active sites, the role of the promoters and also presents some mechanistic considerations.

Keywords: Hydroprocessing catalysis; Molybdate impregnation; Co or Ni ion impregnation; MoS_2; Promoter effect; Active sites

1. Introduction

The hydroprocessing reactions deserve a considerable interest in the petroleum industry as they permit to clean up the different crude oils and distillation fractions which are used as sources of chemicals and/or of fuels. Indeed, petroleum crudes are complex mixtures of hydrocarbons with some other combined elements such as sulphur, nitrogen and also metals like vanadium or nickel in the heaviest molecules identified as porphyrins. At first, the process permits to purify the feeds which are further treated in cracking, hydrocracking or reforming units with catalysts (metals, zeolites) that are very sensitive to poisons. Schematically, in a second step, an important function of hydrotreating catalysis is to improve the quality of the products (gasolines, gasoils and fuels) distributed by the petroleum companies. They must have more and more drastic specifications, namely those relative to environmental and human health protections. The emissions of SO_2 and NO_X upon combustion of fuels have to be considerably reduced by the end of this century.

The hydroprocessing reactions are therefore classified as hydrodesulphurization (HDS), hydrodenitrogenation (HDN) and hydrodemetallation (HDM). In some cases (treatment of fuels from coals), one can also consider hydrodeoxygenation (HDO). In the modern concepts of refining, other reactions are also required during hydroprocessing; they are hydrocracking (HDC), hydrodearomatization (HDA) or hydrogenation (HYD) in general and isomerization (ISOM).

Depending on the nature of the petroleum crude (i.e., light from Middle East or heavy from Vene-

*Corresponding author. Tel.: 33 320 434538; fax: 333 20 436561; e-mail: Jean.Grimblot@univ-lille1.fr

0920-5861/98/$32.00
PII S0920-5861(98)00042-X

zuela), on the feed to be treated, on the refinery capacity and equipments and on the market demand, the reactions involved and the conditions can be quite different. All the reactions are conducted under H_2 the pressure of which is in the range 20–200 atm and with temperatures up to 450°C. These processes require adapted catalysts which are general formulations schematically written as Co(Ni)–MoS_2–γ-Al_2O_3. Recently, some other elements or other supports have been tested and used but the objectives of this presentation are mainly focused on the conventional formulations. In this chapter, we will successively describe the main hydrotreating reactions, the genesis of the catalysts in the oxide form and their transformation into supported sulphides and the nature and properties of the active phase(s). The role of the promoter, the nature of sites and some mechanistic proposals about the action of the catalysts will be further examined.

2. The hydrotreating reactions

As already mentioned in Section 1, the petroleum crudes are extremely complex. In industrial pilots, real fractions are generally used to test the catalysts, but in most of the academic laboratories, the hydrotreating reactions are conducted with model molecules representative of a class of feed. Such investigations deserve interest because they permit to establish comparisons between catalysts, but the effects of competition between molecules at the active sites are totally ignored.

For HDS, thiols and mercaptans are not considered because they are too easily transformed and the most commonly used reference molecule is thiophene C_4H_4S. It has a rather high stability due to its aromatic character. Fig. 1(a) shows the transformation of thiophene which may conduct to tetrahydrothiophene and to desulphurized molecules like butadiene, butenes (all the isomers) and butane [1]. It clearly appears that the catalyst must have different functions, here, mainly hydrogenation of the aromatic ring and the C–S bond hydrogenolysis. For ''deep HDS'', the reactions which implies desulphurization of heavier molecules, dibenzothiophene (Fig. 1(b)) is chosen as a model [2]. However, alkyl dibenzothiophenes are even less reactive because of steric hindrance around sulphur.

Quinoline (Q), in equilibrium with 1-2-3-4 tetrahydroquinoline (THQ) within the experimental conditions, is converted into denitrogenated compounds as propylbenzene (PB) or propylcyclohexane (PCH) through different paths (Fig. 1(c)). One intermediate molecule formed during Q transformation is orthopropyl aniline (OPA) which is in competition on the catalyst with Q for HDN. This inhibiting effect of Q on aniline decomposition is detrimental to the efficiency of the HDN process: as long as Q or 1-2-3-4 THQ are not completely converted, the transformation of OPA can be neglected [3].

Porphyrin-like compounds are representative of heavy molecules. The aromatic tetrapyrrole ring may complex a large number of metals, namely V and Ni in petroleum crudes. The octaethyl vanadyl porphyrin (Fig. 1(d)) is, in a first step, in equilibrium with a hydrogenated product which conducts through a series of steps to complete destruction of the initial molecule [4]. Contrary to the other reactions which form hydrocarbons and gaseous NH_3 or H_2S, here, badly dispersed vanadium sulphide is deposited on the catalyst surface and may block its porosity [5].

3. Genesis of the catalyst

3.1. Impregnation

The objectives of the catalyst preparation are to well disperse the elements which will participate in the promoted (Co,Ni) active phase (MoS_2) on a support. A transition γ-Al_2O_3 support, usually preformed, with a surface area in the 200–300 $m^2\ g^{-1}$ range, is generally chosen. Its porosity should be adapted to the nature of the feed to be treated. For industrial purposes, the *dry impregnation* or the *pore filling method* is preferred. It consists of using a volume of solution which exactly corresponds to the pore volume of the support. In the solution, the two elements of interest are generally introduced simultaneously, as soluble compounds, in concentrations required to deposit the expected amounts of the respective oxides like CoO, NiO and MoO_3. Alternatively, two sequences of impregnation can be used. The impregnated support is then dried and calcined in air (400°C–500°C) to eliminate water and the other cations (NH_4^+) or anions (NO_3^-) also present in the solution. The pore filling method,

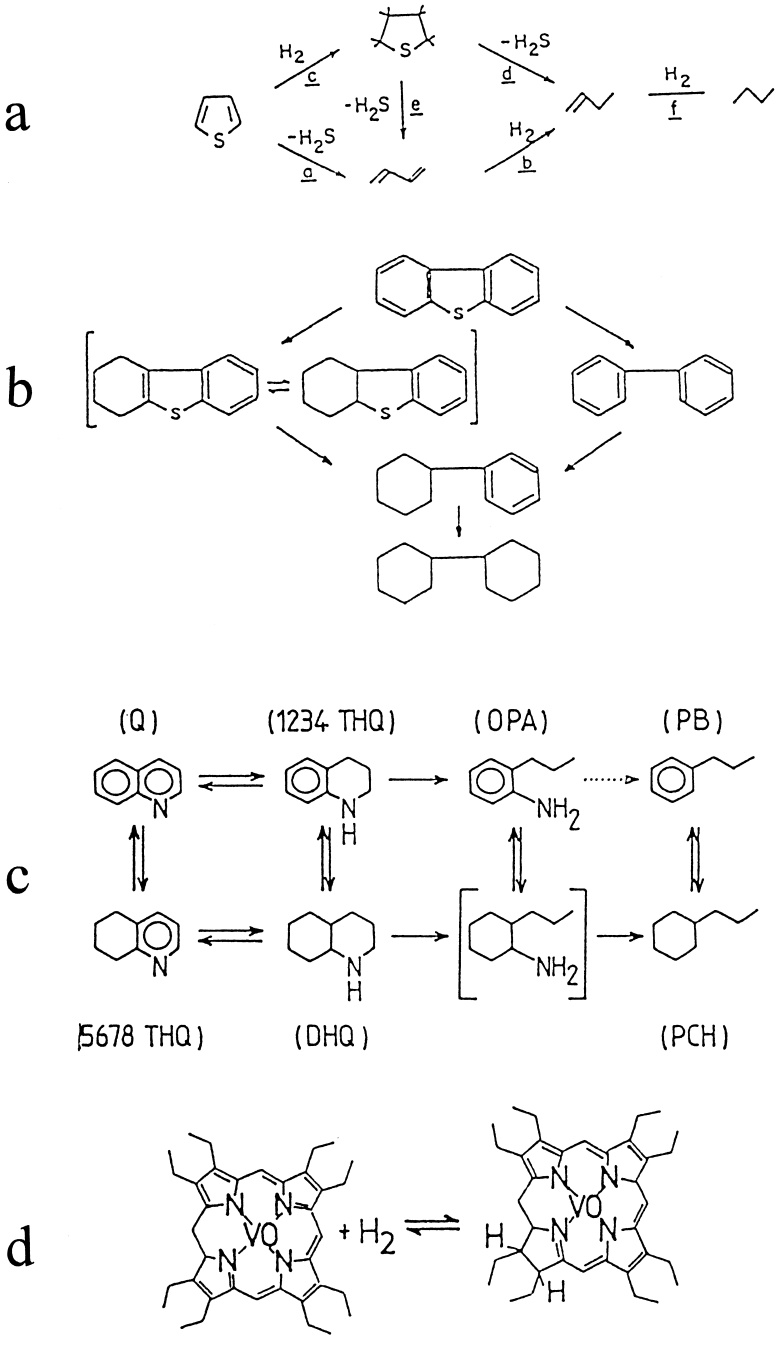

Fig. 1. Model reactions occurring during hydrotreatment: (a) HDS of thiophene (from Ref. [1]), (b) HDS of dibenzothiophene (from Ref. [2]), (c) HDN of quinoline (from Ref. [3]), and (d) Hydrogenation equilibrium of vanadyl octaethyl porphyrin (from Ref. [4]).

which requires optimization, is industrially used as it avoids eliminating large volumes of water in the drying step, a step energy consuming.

In the laboratory scale, the *equilibrium impregnation method* is sometimes preferred as it permits to modify and adjust several parameters (nature and pH of the solution, concentration, temperature, time to reach equilibrium...) in order to have a better understanding of the interactions which exist between the species in solution and the surface of the support. After drying and calcination, the obtained samples are classically labelled as $CoO(NiO)–MoO_3–\gamma\text{-}Al_2O_3$. This does not imply the presence of separate oxide phases in the catalysts.

In the following, the focus will be on results obtained either by the equilibrium or by the pore filling methods. Let us consider first the *impregnation of molybdenum*. $\gamma\text{-}Al_2O_3$, in suspension in aqueous solutions, tends to be electrically charged, like other mineral oxides, and it has been suggested that the mechanisms of impregnation are mainly driven by electrostatic forces at the solution–solid interface [6]. At the isoelectric point (IEP), pH at about 8 for alumina, the solid is globally neutral. For pH below IEP the particles of the solid are positively charged and vice versa. For alumina, the equilibria are, respectively,

$$Al-OH + H^+,\ A^- \leftrightarrow Al-OH_2^+,\ A^- \quad pH < IEP$$

$$Al-OH + B^+,\ OH^- \leftrightarrow Al-O^-,\ B^+ + H_2O \quad pH > IEP$$

Ammonium heptamolybtate (AHM or $(NH_4)_6Mo_7O_{24}$) is generally the source of molybdenum for preparing the impregnating solutions. NH_4^+ ions are preferred to alkaline ones as it can be easily decomposed during the subsequent calcination step whereas Na^+ or other, if adsorbed, may modify the surface properties of the alumina support. In molybdate solutions, condensation–decondensation reactions occur with the most important equilibrium, as

$$Mo_7O_{24}^{6-} + 4H_2O \leftrightarrow 7MoO_4^{2-} + 8H^+$$

Other ions, like $Mo_8O_{26}^{4-}$, in lower amount, are not considered. The interesting features are that the equilibrium is pH dependent and the Mo-containing species are always negatively charged. From Tsigdinos et al. [7], the natural pH of AHM solutions varies between 5.1 and 5.5 depending on the concentration, with heptamolybdate as the major species. At such a pH, the alumina surface is positively charged and consequently electrostatic attraction favours adsorption of the molybdate species. The adsorption phe-

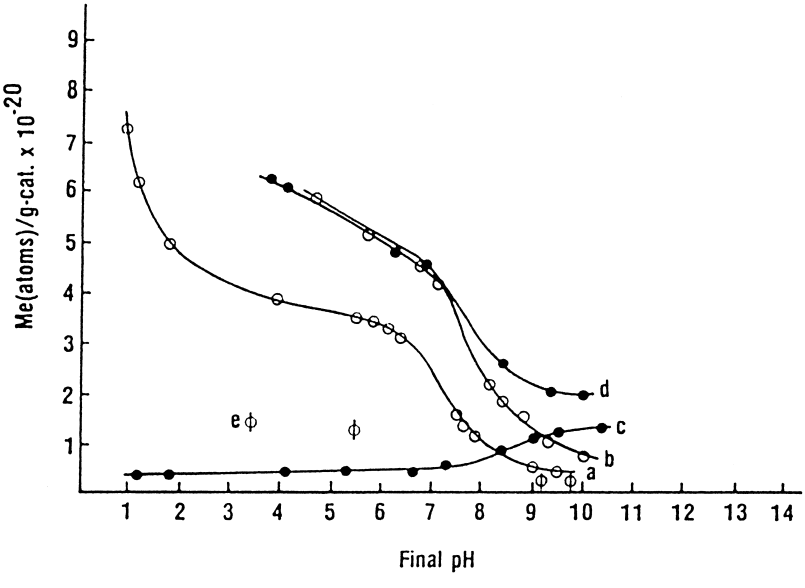

Fig. 2. Amount of ions adsorbed on γ alumina at equilibrium as a function of the final pH of the adsorbate solution: (a) molybdate, (b) tungstate, (c) Na^+, (d) vanadate, (e) chromate (reproduced with kind permission of Academic Press, from Ref. [8])

nomenon is clearly evidenced in Fig. 2 (part (a) for molybdates) which represents the amount of ions deposited on alumina at equilibrium (the alumina-solution suspensions were shaked up to 100 h) as a function of pH [8]. At high pH, the amount of adsorbed molybdate is very low whereas a pseudo plateau is obtained between pH 2 and 6. At the lowest pH, precipitation inside the pores of alumina occurs to produce ill-dispersed species, precursor of MoO_3. This region is not representative of an equilibrium adsorption. Note also that the response for Na^+ is just opposite to the anionic species. Such equilibrium results have been confirmed by Kasztelan et al. [9] who showed that the small amount deposited at pH 11 is easily removed by water washing. This is a confirmation of the weak interaction between molybdate and the γ-alumina surface at pH higher than that of the IEP of the support. Liquid phase nuclear magnetic resonance (NMR) of ^{95}Mo allowed characterization of the molybdenum solutions inside the pores of the support during impregnation [10,11]. In pure solutions at natural pH, the NMR spectra depend on the AHM concentration (Fig. 3(A)). They show the presence of MoO_4^{2-} (chemical shift ∼0) and $Mo_7O_{24}^{6-}$ (shift ∼35 ppm), the latter species being quickly dominant when the Mo concentration increases. In the presence of γ-Al_2O_3 (pore filling impregnation method), the solution remaining in the pores does not show the presence of heptamolybdate for a wide range of Mo loading (Fig. 3(B)).The single peak observed is attributed to MoO_4^{2-}. The shoulder detected at a concentration corresponding to a deposition of 35 wt% of MoO_3 is due to the heptamer. Quantitative estimation of the amount of Mo remaining in solution in the pores of alumina revealed that more than 97% of Mo initially present is adsorbed on the solid and therefore, not detected by liquid NMR [12]. The strong interaction between the molybdates in solution with alumina at pH below IEP is once again demonstrated.

Extensive characterizations [8,9,12–19] by laser Raman spectroscopy (LRS) have permitted to investigators identify the nature of the deposited molybdate(s) on the alumina support and to follow their transformation during the successive steps of drying to remove water from the pores of the support and calcination in air up to about 500°C in general for decomposing NH_4^+ (or other ions as already mentioned), and for strengthening the bonds between the Mo-oxo-species with the support.

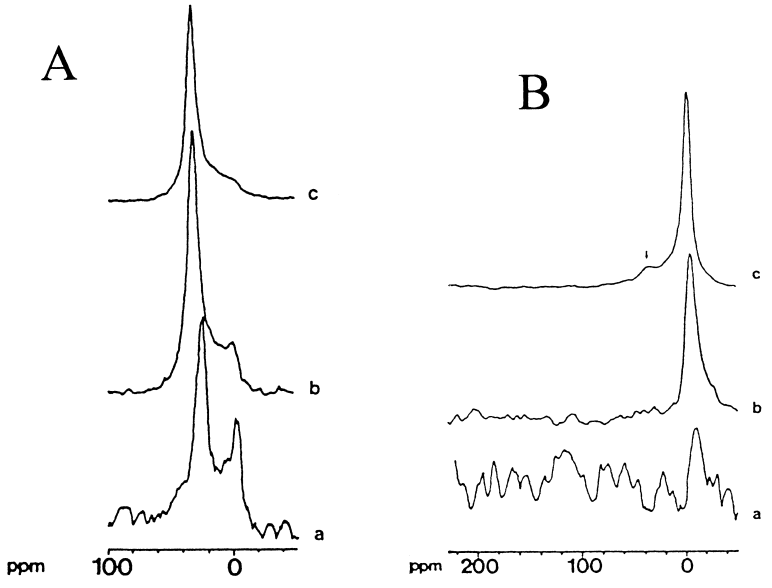

Fig. 3. (A) ^{95}Mo NMR spectra of ammonium heptamolybdate solutions at natural pH: (a) 0.07 M; (b) 0.3 M; (c) 0.7 M. (B) ^{95}Mo NMR spectra of ammonium heptamolybdate solution in the pores of γ-Al_2O_3: (a) 1.8 wt% MoO_3; (b) 14 wt% MoO_3; (c) 40 wt% MoO_3 (reproduced with kind permission of American Chemical Society, from Ref. [11]).

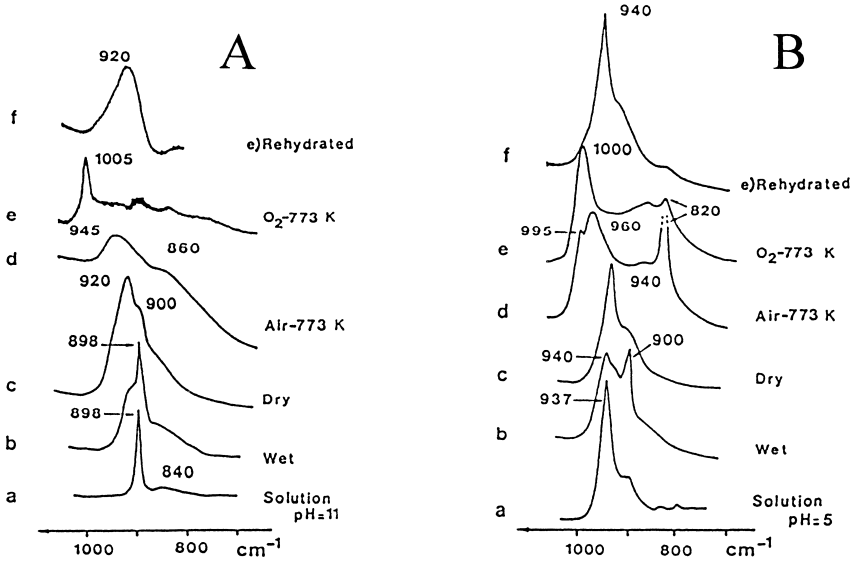

Fig. 4. Raman spectra evolution during preparation of MoO_3–Al_2O_3 catalysts: (A) Evolution from the solution at pH 11, containing the monomer MoO_4^{2-}, to a 4 wt% MoO_3–Al_2O_3 catalyst. (B) Evolution from the solution at pH 5, which mainly contains $Mo_7O_{24}^{6-}$, to a 14 wt% MoO_3–Al_2O_3 catalyst (reproduced with kind permission of American Chemical Society, from Ref. [19]).

MoO_4^{2-} (M), a perfect tetrahedral species in solution, has the major Raman band at 898 cm^{-1} (Fig. 4 A(a)) whereas the main band of the heptamer (HM) which contains distorted MoO_6 octahedra is at 937 cm^{-1} (Fig. 4 B(a)). In the low wave number region, some differences are also noted: 316 cm^{-1} for M, 357 and 217 cm^{-1} for HM. Supported monomeric species can be obtained for Mo amounts lower than 5.5 wt% MoO_3 or about 1 Mo atom nm^{-2} on a 250 $m^2\,g^{-1}$ alumina support [19]. Part A of Fig. 4 shows the spectra evolution of a catalyst loaded (pore filling impregnation) with 4 wt% MoO_3. The wet impregnated support gives a Raman spectrum (Fig. 4 A(b)) similar to M in solution. This result shows that transformation of HM into M has occurred during wetting the support. Upon drying and calcination in air, first shifts to 920 cm^{-1} and then to 945 cm^{-1} are evidenced (Fig. 4A(c) and (d)). It has been assumed [19] that this bound molybdate species is only completely dehydrated by calcination in O_2 at 773 K. Rehydration conducts, reversibly, to the band at 920 cm^{-1}, which is the bound monomer whose local environment is modified by thermal treatment. The evolution of HM during the preparation of a 14 wt% MoO_3 catalyst is presented in Fig. 4 B. On the wet sample, both M (900 cm^{-1}) and HM (940 cm^{-1}) are detected (Fig. 4 B(b)). Upon calcination, presence of bulk MoO_3 (intense bands at 995 and 820 cm^{-1}) is detected. Besides that presence, a band at 960–970 cm^{-1} and a broad shoulder at 850 cm^{-1} are characteristic of a bound polymolybdate phase. Therefore, the main conclusion from these studies is the presence of poly-oxo-molybdate structures in a wide range of Mo content; only the less loaded samples may contain monomeric species. All the supported entities are influenced by water in their coordination sphere.

Fourier Transform IR spectroscopy for characterizing the OH groups of alumina in association with other techniques has shown interesting results related to the interaction of molybdates with the support [12]. Two mechanisms of interaction between the oxo-molybdenum species and alumina are described for Mo loadings up to 3.7 Mo atoms nm^{-2} and discussed in the light of other results [20–22]. Basic OH groups of alumina are implied in the heptamer fixation up to 2 Mo atoms nm^{-2}. Between 2.0 and 3.7 Mo atoms nm^{-2}, another deposition mechanism applies in which the residual basic OH groups, as well as other OH groups, do not participate. The reactive basic hydroxyls are progressively removed by grafting Si

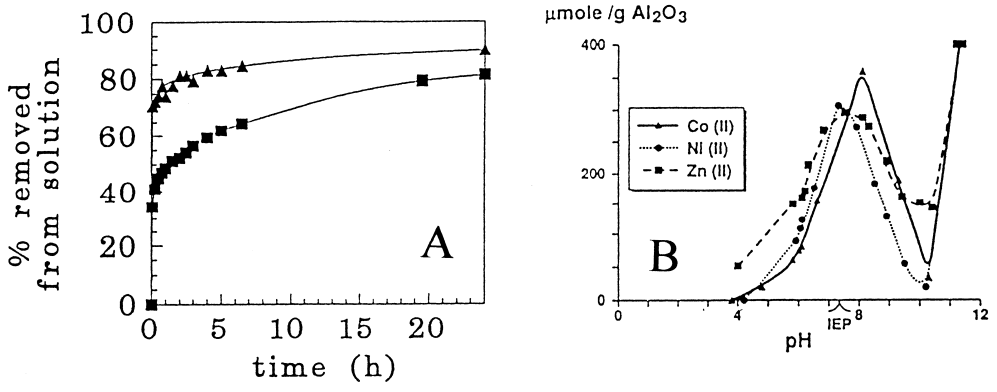

Fig. 5. (A) Ni (lower curve) and Co (Upper curve) uptakes by γ-alumina as a function of time (reproduced with kind permission of American Chemical Society from Ref. [26]). (B) Adsorption of Co(II), Ni(II) and Zn(II) ammine complexes on γ-alumina as a function of pH of the impregnating solution (contact time=3 h, room temperature) (reproduced with kind permission of Elsevier Science, from Ref. [25]).

on alumina with tetraethoxysilane (TEOS). The loading of 3.7 Mo atoms nm^{-2} corresponds to the limit of monolayer coverage for the alumina used in this work [12]. Such a limit has been evidenced by X-ray photoelectron spectroscopy (XPS) or by ion scattering spectroscopy (ISS). On other transition aluminas, the monolayer limit could be slightly different but never exceeds 5 Mo atoms nm^{-2}.

Thus, *in short*, impregnation of γ-alumina by molybdate solutions and the further drying and calcination steps conduct to well dispersed poly-oxomolydates with no or minor amount of isolated species bound as tetrahedral molybdate when the conditions of preparation are correctly chosen. Presence of bulk MoO_3 and of $Al_2(MoO_4)_3$ has to be avoided as they are not good precursors for getting the dispersed active MoS_2 phase. Crystallites of bulk MoO_3 , easily revealed by X-ray diffraction (XRD) or LRS, are obtained after the monolayer limit and $Al_2(MoO_4)_3$ is formed for temperatures of calcination largely higher than 500°C.

The *interactions of solutions containing* Co^{2+} *or* Ni^{2+} *ions with alumina* is far less documented than for deposition of molybdates. In the early work of Grimblot et al. [23], XPS measurements revealed that the Co^{2+} ions are occupying tetrahedral surface sites of alumina up to about 3 Co atoms nm^{-2} (impregnation of alumina–100 $m^2\ g^{-1}$–with excess of cobalt nitrate solution and evaporation of excess of water). After the monolayer has been formed, heterogeneous Co_3O_4 appears. When comparing impregnation of alumina by Ni^{2+} or Co^{2+} ions from nitrates in aqueous solution [24] in the monolayer range, the cobalt species were identified as Co^{2+} in tetrahedral sites located just below the support surface, whereas a $NiAl_2O_4$ surface spinel was present with a high octahedral site occupation by Ni^{2+} ions. In addition, with Ni, no bulk NiO nor $Ni(OH)_2$ compounds were formed. More recently, Clause et al. [25,26] have studied in detail the phenomena occurring during impregnation of γ-Al_2O_3 by Co(II), Ni(II) and Zn(II) species in aqueous solutions. They found, in particular, that γ-alumina is not as inert as expected even under mild conditions, i.e. room temperature and pH values around IEP of alumina. The impregnating solutions contained the respective Co or Ni nitrates and also ammonium nitrate, to ensure ammonia complexation of the ions and to avoid precipitation of hydroxides; pH was adjusted by bubbling gaseous ammonia. Fig. 5(A) shows the Ni and Co uptakes at pH 7.2 (Ni) or 8.1 (Co).The relative deposition rate order was found to be Co(II)>Ni(II)>>Zn(II) and is independent of the tested γ-alumina. After a contact time of 24 h, about 80% of ions are removed from solution. Provided that larger contact times are used, up to two weeks, the ions are quantitatively removed from the solutions; this means that at equilibrium, the concentrations in solution are negligible. Fig. 5 (B) shows the amount of adsorbed Co(II), Ni(II) or Zn(II) amine complexes as a function of pH for a contact time of 3 h at room temperature. The most significant result is the presence of a maximum at pH values close to the IEP of the support. This suggests

that interaction with alumina in this intermediate pH range is not simply electrostatic. Indeed, several techniques like XRD or EXAFS (extended X-ray absorption fine structure) patterns have shown the presence of coprecipitate compounds associated with Al(III) and with the hydrotalcite-type structure like $[M(II)_2 Al(OH)_6](NO_3), H_2O$. Such compounds are already present in the wet impregnated solids; drying has no significant effect on the formation of coprecipitates. The mechanism of their formation seems to involve a dissolution–reprecipitation process with breaking of Al–O–Al bonds in the surface region of alumina.

Simultaneous deposition of Co (*or* Ni) *with molybdate* on alumina is the easiest and cheapest way to prepare the catalyst, provided that the respective Co and Mo containing compounds and their amounts are compatible for preparing a unique impregnation solution (i.e., complete dissolution and no coprecipitation). Samples obtained by simultaneous deposition are often compared to those prepared by successive impregnation with Mo first or vice versa, with main characterizations by XPS and ISS to provide informations on the relative dispersions of the two elements Co–Mo or Ni–Mo and on their possible interactions. The results are rather contradictory in the literature probably because many preparation conditions are used. Let us only focus attention on some conclusions. Early in 1976, Mone [27] proposed a model for NiO–MoO_3–Al_2O_3 oxide catalysts in which the Ni^{2+} ions are deposited on a molybdate layer if calcination does not exceed 773 K, with no formation of $NiAl_2O_4$. More recently, Knözinger and coworkers [28,29] showed that: (i) Ni^{2+} was partly incorporated within the monolayer molybdate with preferred occupation of octahedral sites, (ii) the remaining Ni^{2+} are located in an aluminate matrix with no, or eventually very few, occupation of tetrahedral sites, (iii) the extent of Ni^{2+} reduction depends on the amount of Ni present in the molybdate layer; Ni^{2+} also facilitates reduction of Mo(VI) oxo-species and (iv) the distribution of Ni^{2+} between the molybdate layer and the support to form an aluminate depends very strongly on the sequence of impregnation, calcination time and temperature. At 870 K, there is a spreading of the molybdates over the support surface and diffusion of Ni from the molybdate layer to the bulk alumina matrix.

In their investigation, Kasztelan and coworkers [18] have shown that a part of the promoter diffuses into the support by calcination. The rest, in a strong interaction with the supported molybdate phase, modifies its hydration–dehydration properties which have been revealed in Fig. 4. Moreover, ISS experiments [30] clearly evidenced a strong shielding effect of the Mo element by the promoter Co or Ni. That observation is a direct proof of a chemical interaction between the promoter and the oxo-molybdenum supported species; such an interaction is described by the possible formation of isopolymolybdate salts of Co or Ni.

More recently, co-deposition of Mo(VI) species and Co^{2+} [31] or Ni^{2+} ions [32] on γ-alumina using an equilibrium deposition followed by filtration (EDF) has been studied in slightly acidic solutions. It has been shown, in particular, that strong lateral interactions exist between the adsorbed Mo(VI) species and Ni^{2+} or Co^{2+} ions present in the inner Helmholtz plane (HIP) developed between the support surface and the impregnating solution (Fig. 6). This strong interaction favours the mutual promotion of deposition by EDF of Mo(VI) and Ni^{2+} and also prevents a

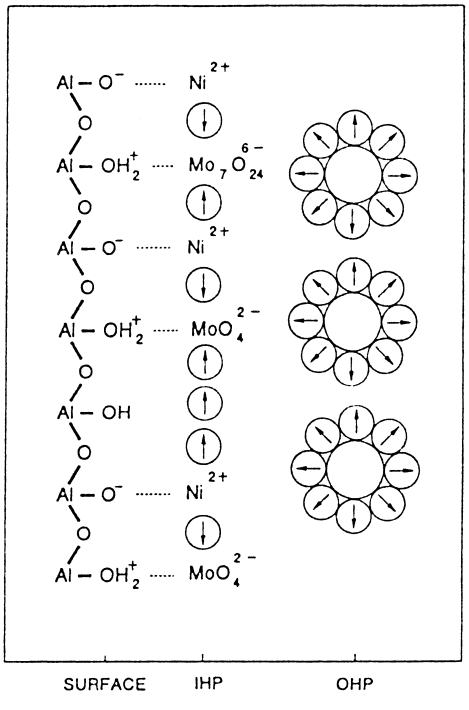

Fig. 6. Schematic representation of molybdates and Ni^{2+} ion codeposition on the γ-alumina surface. IHP and OHP mean, respectively, inner and outer Helmholtz planes. (reproduced with kind permission of Academy Press, from Ref. [32]).

strong interaction between Ni^{2+} and the alumina surface. As a consequence, the formation of catalytically inactive $NiAl_2O_4$ can be inhibited.

In short, the choice of key parameters during deposition of Mo and promoters as well as the calcination temperature of the impregnated support should develop a surface phase associating Ni or Co in/on the molybdate phase and reduce the formation of surface or bulk $NiAl_2O_4$ or $CoAl_2O_4$ spinels which are not desired for catalysis. Presence of bulk $CoMoO_4$ or $NiMoO_4$ is not desired as well. However, it has also been shown that a part of Ni located in a surface aluminate can be mobile enough during the sulphidation step to migrate and promote (at least in part) the MoS_2 active phase [33]. On the one hand, recent preparation procedures [34–36] have shown that adding complexing agents in the impregnation solution can really modify the catalytic properties of such systems which means that the interaction Ni–Mo or Co–Mo has been optimized. For example, a Co–Mo catalyst prepared using citric acid is superior to the similar system using ammonia in terms of HDS activity [34]. On the other hand, the use of ethylenediamine (EDA) improves the Mo dispersion, avoids formation of unwanted crystallites of Co_3O_4 or $CoMoO_4$ and provokes an increase of thiophene HDS activity per gram of catalyst [35].

3.2. Synthesis by sol–gel methods

In the recent years, we used sol–gel derived methods to prepare Mo-based hydrotreating catalysts [37,38]. Pure alumina can be prepared first by controlled hydrolysis of aluminium alkoxide precursors to conduct to powders after solvent elimination and calcination. These materials could be the basis of catalyst supports or ceramic precursors. Such preparations have been extensively studied in the literature and will not be further examined in this review. Let us notice only that alumina synthesis by using sol–gel procedures can produce a very large variety of samples with adapted porosity and structure (from rather amorphous to well-defined α-alumina, depending on the sintering temperature used) and with high purity.

Such high surface area supports can be impregnated by solutions containing molybdates and eventually other soluble salts and for which apply the previous descriptions and discussion. Conversely, during the sol–gel procedure, the elements of interest for hydroprocessing catalysts (Mo, Co, Ni...) can be added at some selected steps. For example, the molybdenum oxo-species can be dispersed in butanediol and added to the aluminium tri sec-butylate solution before hydrolysis [38]. With impregnated alumina prepared by a sol–gel procedure (initial surface area-$=423\ m^2\ g^{-1}$), the amount of deposited Mo in a monolayer range can be as high as 28 wt% in Mo (limit at which MoO_3 is detected). For the highest loaded sample, the surface area keeps high values to about $280\ m^2\ g^{-1}$. With the procedure using incorporation of molybdenum during the gel synthesis, it has been shown [38] that the solids contain well dispersed molybdates in tetrahedral and octahedral environments with Mo loadings up to 30 wt% in Mo. This series of samples exhibits high surface area in the 400–$500\ m^2\ g^{-1}$ range. The Mo oxo-species are probably incorporated in the very open framework of alumina. Fig. 7 shows the results of thiophene HDS conversion on three series of sulphided Mo alumina catalysts which permit comparison of the different preparation procedures. The reference series, noted I in Fig. 7, concern samples of a commercial alumina impregnated classically (dry impregnation). The series concerning the impregnated sol–gel alumina noted SGI, exhibits a conversion evolution curve as a function of the Mo loading quite similar to the I series with, however, a maximum activity at 24 wt% Mo instead of 17 wt% Mo. At these maxima, thiophene conversion is much efficient for the SGI samples. These results show that impregnation of a sol–gel alumina allows to increase the loading of Mo in a well dispersed precursor state. The behaviour of samples prepared by direct incorporation of Mo in the sol–gel procedure, samples noted SG in Fig. 7, is different as the activity keeps on increasing in the whole range of Mo loading up to 30 wt% Mo. In the conditions used, 50% thiophene conversion per gram of catalyst (part a of Fig. 7) can be reached instead of about 25% at the maximum of the reference series. Part (b) of Fig. 7 shows, for comparison, the evolution of activity per gram of Mo present in the different catalysts.

3.3. Sulphidation of the oxidic precursors

The oxidic precursors, after the calcination step, are transformed by sulphidation treatments into the active

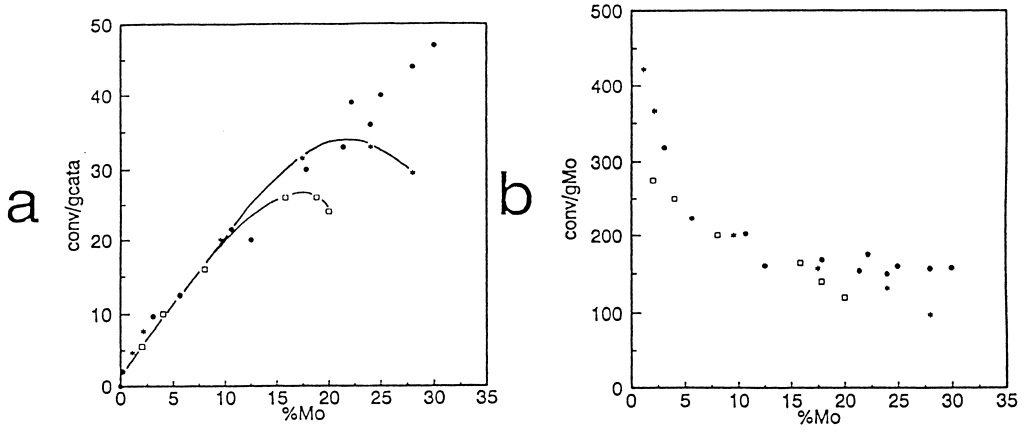

Fig. 7. Evolution of thiophene HDS conversion as a function of the Mo loading for three series of sulphided Mo-alumina catalysts: ★- SGI impregnated sol–gel alumina.●-SG, Mo incorporated during the sol–gel procedure.□-I, impregnated commercial alumina. Part (a): conversion per gram of catalyst. Part (b): conversion per gram of Mo (reproduced with kind permission of Kluwer Academy Publishers, from Ref. [38]).

form of the catalyst. In some industrial practices, presulphidation of the catalysts is carried out, first by deposition (adsorption?) of molecules containing sulphur on the precursor outside the refinery plant and, in a second step, the presulphided catalysts placed in the hydroprocessing reactor are activated by H_2 (Sulficat® process). In the laboratory scale, the processes are generally conducted directly from the oxidic precursors under a flowing mixture associating a reductive agent (H_2) and a sulphiding molecule such as H_2S, dimethyldisulphide, CS_2 or thiophene. These processes, extremely complex at a molecular scale, have been considerably studied and only some major aspects will be considered here. Interesting information comes from the work of Moulijn and coworkers [39–41] who used a very efficient technique called temperature-programmed-sulphiding (TPS), to continuously follow the H_2S, H_2O and H_2 concentrations in a H_2S/H_2/Ar mixture interacting with a catalyst as a function of temperature or time. As an illustration, Fig. 8 shows two typical TPS patterns of a MoO_3–Al_2O_3 catalyst containing 4.5 Mo atoms nm^{-2} and pretreated in Ar at room temperature [part(a)] or at 775 K [part(b)]. The evolution is quite different from bulk compounds, i.e. MoO_3, MoO_2, which are sulphided with more difficulty. On the catalyst pretreated at room temperature, in 320–450 K range, H_2S is trapped by the catalyst in large quantities with a rather identical H_2O production pattern slightly shifted in temperature. No H_2 consumption is found below 400 K. At around 500 K, H_2 is consumed (sharp peak) while H_2S is simultaneously produced. At higher temperature, H_2S is consumed again with production of H_2O. Calibrations indicate that ~1.0 H_2 and 1.9 H_2S molecules are consumed per Mo. Pretreatment of the catalyst at 775 K leads to a broadening and shift of the TPS pattern to higher temperatures. Evidently, water in the coordination sphere of the supported poly-oxomolybdate has an effect on the sulphidation process. On the other hand, the increase of the Mo loading in 0.5–4.5 Mo atoms nm^{-2} range leads to sulphidation at lower temperature but the effect is not very pronounced. TPS of CoO–MoO_3–γ-Al_2O_3 catalysts [41] shows that sulphidation occurs at lower temperature than bulk compounds such as MoO_3, CoO or $CoMoO_4$. The latter helps to separate the MoS_2 and Co_9S_8 phases. Sulphidation of cobalt strongly depends on the calcination temperature of the precursor; $CoAl_2O_4$, when present, is sulphided only around 1050 K.

Sulphidation of MoO_3-γ-alumina catalysts has also been followed by in situ laser Raman spectroscopy [42]. The process has been found very complex and depends on the hydration state of the oxidic precursor, on the nature of the sulphidation mixture (H_2/H_2S or N_2/H_2S) and also on temperature and duration of the treatment. Intermediate compounds like oxysulphides (S/O exchange in the polymolybdate) have been

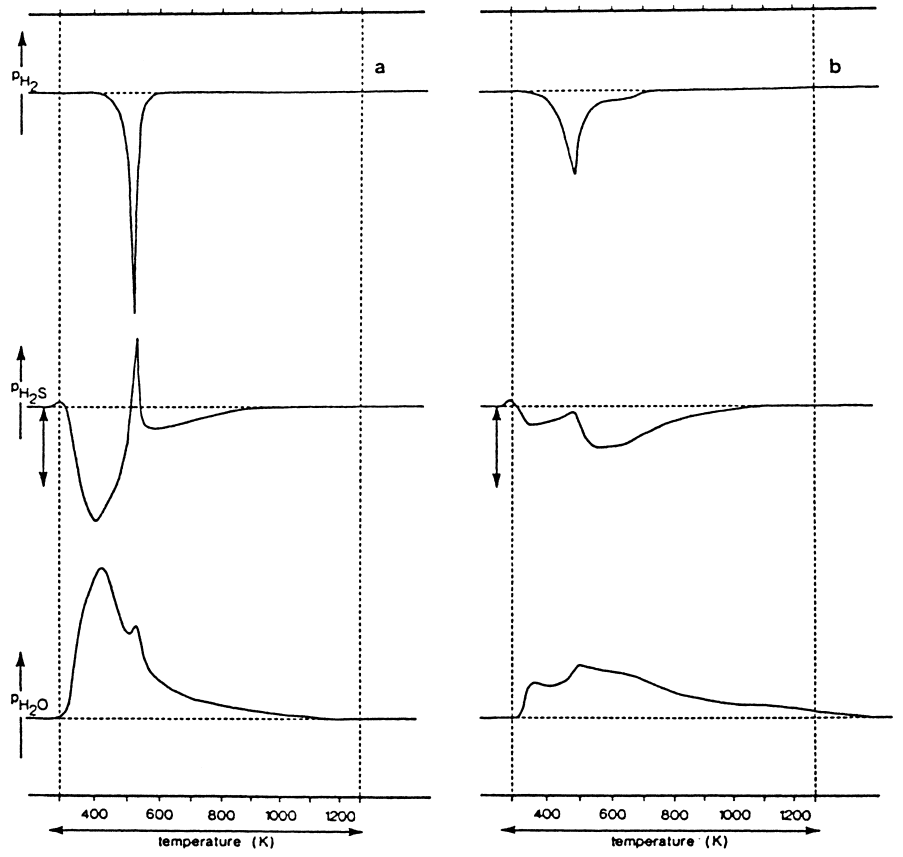

Fig. 8. TPS pattern of a MoO_3 (4.5 Mo atoms nm^{-2})-Al_2O_3 catalyst pretreated in Ar at (a) room temperature, (b) 775 K. The double vertical arrow indicates the 50% conversion level of H_2S (reproduced with kind permission of Academy Press, from Ref. [39]).

identified. Nevertheless, the final compound appears to be always MoS_2 (two characteristic bands at ~385 and 408 cm^{-1}) with, depending on the conditions, possible intermediate formation of MoS_3 (Fig. 9).

In general, more than 90% of Mo in the oxidic precursor is transformed during sulphidation into a MoS_2 supported state. MoS_2 is a natural compound (molybdenite) which has a layer structure. The weak van der Waals interaction between two successive layers (Mo–Mo distance=6.15Å) gives interesting lubricating properties to MoS_2. Within the MoS_2 layer, Mo(IV) is bound to six sulphur ions (S^{2-}) in a trigonal prismatic coordination with respectively, 2.41 and 3.16 Å for the Mo–S and Mo–Mo distances [43]. Three dimensional MoS_2 may have well organized hexagonal (Fig. 10) [44] or rhombohedral structures or, essentially when it has been prepared at low temperature, a very disordered architecture. On supports like γ-alumina, investigations by EXAFS or high resolution electron microscopy (HREM) have shown that the MoS_2 phase is mainly made of very small crystallites or platelets having the MoS_2 intrinsic structure with, however, no or very few layer stacking. In a HREM study of the morphology of MoS_2 catalysts on different supports, Payen et al. [45] have established diagrams reporting the lengths L and the numbers N of stacked layers from observations of more than 400 crystallites. Mean L and N values can be calculated from the results. For a 14 wt% MoO_3 on alumina, (impregnation by the pore filling method) sulphided at 623 K by H_2S/H_2 (10/90) the histograms show that L never exceeds~8.0 nm and N maximum is 3–4; the majority is single layer crystallites. The mean values are respectively, 3.5 nm (L) and 1.4 layers (N).

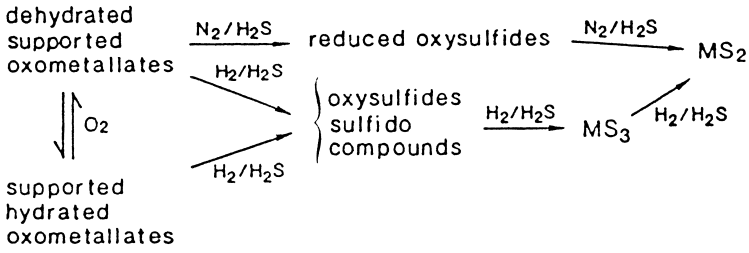

Fig. 9. Schematic transformation of MoO_3-alumina by sulphidation (from Ref. [42]).

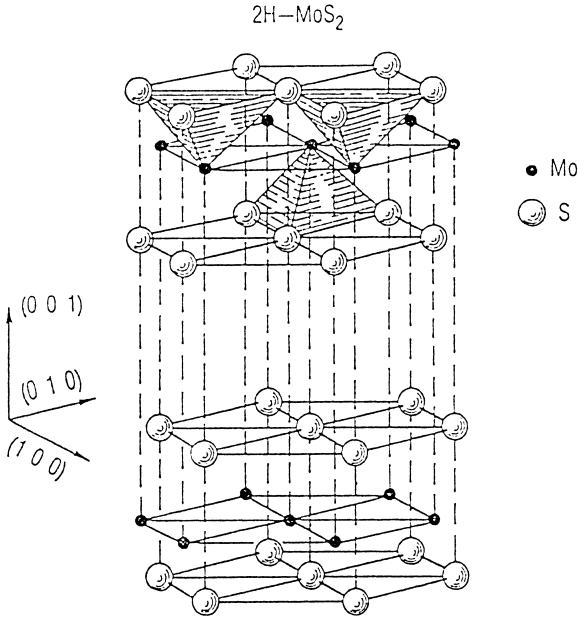

Fig. 10. 2H–MoS_2 hexagonal structure showing the S–Mo–S sandwiches and the interlayer or Van der Waals gap. This picture is taken from several papers published by The Aerospace Corporation, namely in Ref. [44].

Data in this range of values have been very often found in the literature [46–48] and references cited in [45] and are considered to correspond to a well dispersed MoS_2 phase. On the contrary, on supports other than γ-alumina, larger crystallites can be found.

Contrary to MoS_2, the presence of crystallites of promoter sulphides as Co_9S_8 or NiS_x in separate phases are not easily detected by HREM. However, in case of cobalt containing catalysts, either bulk or supported, Mössbauer emission spectroscopy (MES) is a very convenient technique to identify the local environment of this promoting element. Model compounds such as cobalt incorporated in alumina ($Co:Al_2O_3$), cobalt in sulphided phases like Co_9S_8, CoS_2, Co_3S_4 or CoS_{1+x}, Co metal and $CoMo_2S_4$ exhibit very different MES patterns which can be used as fingerprints for identifying the state of cobalt in the sulphided Co–MoS_2 catalysts [49–53]. When preparing a series of Co–MoS_2 samples which were further examined by MES, Topsøe and coworkers found a quadrupole doublet which was not observed in any spectra of the cobalt sulphides or in $CoMo_2S_4$ and this particular species was assigned to cobalt in the so-called "Co–Mo–S" phase which was considered to be the effective promoted active phase. On Fig. 11 (part A) are reported the ME spectra of CoO–MoO_3–η-Al_2O_3 catalysts (two sequences of impregnation, 8.6 wt% Mo, doped with ^{57}Co) with different Co/Mo atomic ratio and sulphided at 625 K in a flow of 2% H_2S in H_2. The spectra have been decomposed into three components which correspond to the promoted Co–Mo–S phase, to Co_9S_8 and to Co in alumina. The relative amount of Co–Mo–S decreases from 89% (Co/Mo=0.09) to 20% (Co/Mo=1.19). The Co repartition can be compared to the catalytic activity data (part B of Fig. 11). When Co_9S_8 becomes largely dominant, the catalytic activity tends to decrease. Therefore, although Co_9S_8 is the major phase at high Co loadings, its presence is not essential for promotion.

The correlation between catalytic activity performances and the presence of cobalt in intimate contact with MoS_2 appears quite unambiguous and has also been revealed with the Ni–MoS_2 system. However, other authors have found [54–57] MES similarities between Co species in either Co or Co–Mo sulphides supported on carbon or on alumina. It turns out that the quadrupole splitting of highly dispersed cobalt sulphides is similar to that found in the Co–Mo–S phase

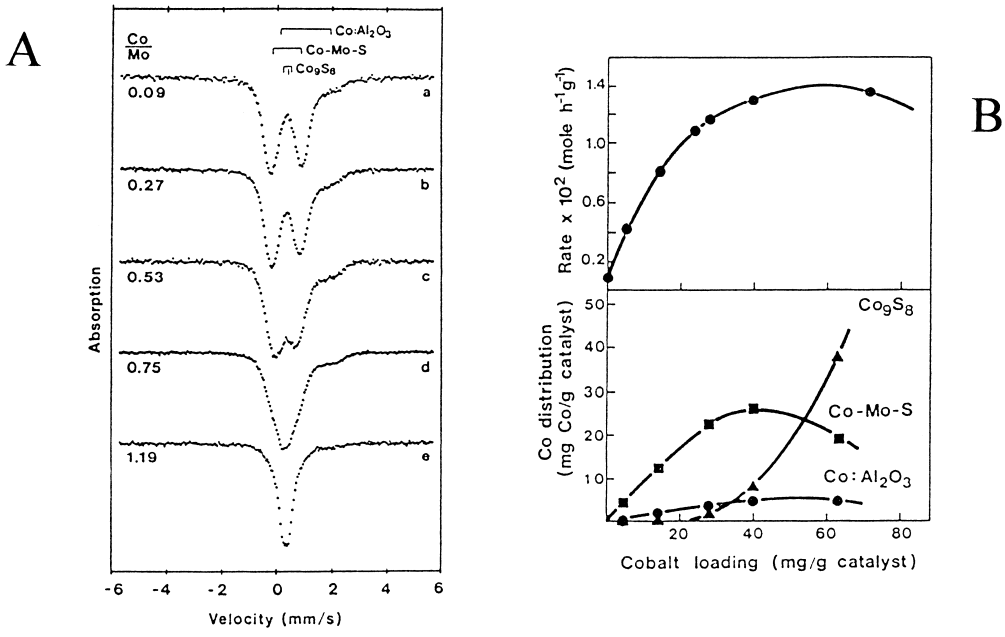

Fig. 11. (A): In-situ Mössbauer spectra obtained at 300 K of sulphided catalysts with different Co/Mo ratios (from Ref. [50]). (B): Relative distribution of cobalt in three different environments and activity evolution during thiophene HDS (reproduced with kind permission of Academic Press, from Refs. [50] and [53]).

and, as a consequence, the presence of the latter could not be as general as assumed by the group of Topsøe. Moreover, Vissers et al. [58] found that the intrinsic activity for thiophene HDS in Co on carbon catalysts without Mo is comparable to that of the Co–Mo–S phase in mixed Co–Mo/C catalysts.

In short, after sulphidation, HREM reveals the presence of platelets of MoS_2 which can effectively interact with Co species in the so-called Co–Mo–S phase, but presence of very small crystallites of well dispersed Co sulphides as well as sulphided Mo species not detected by microscopy cannot be ruled out. Their presence could noticeably and positively affect the catalysts performances.

4. Nature of sites, role of promoters and mechanistic aspects

4.1. *Sites associated with* MoS_2

MoS_2, the main active phase in hydrotreating catalysts, has a highly anisotropic layered structure (Fig. 10) which allows to distinguish between basal and edge planes. In stacked crystallites, the van der Waals interactions between two successive basal planes are so weak that it is possible to consider only one single layer. As HREM revealed that the supported platelets are very small, the two-dimensional (2D) structure within one layer is limited by edges with broken or dangling Mo–S bonds which should exhibit much higher reactivity than the rather inert basal plane. Numerous investigations in the literature have tried to evidence specific reactivity of edges with molecules or metallic species (O_2, Co, see for example [59]). To confirm the importance of the edges of the MoS_2 platelets in hydrotreating catalysts, a geometrical visualization and modelling has been proposed [60]. Fig. 12 reports two possible models of MoS_2 single slabs as being completely sulphided rhombohedral or hexagonal fragments of 2D-MoS_2: the different locations of Mo and S atoms at basal, edge and corners can be easily recognized and their respective proportions calculated as a function of the size or, in other words, of the total number of Mo in a single crystallite. Note, in particular, that Mo at the edges can

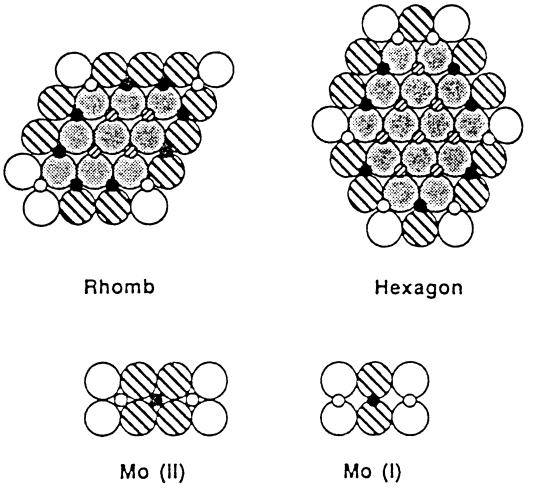

Fig. 12. Top view of modelled MoS_2 single layer crystallites and side view of the two possible Mo locations at the edges (reproduced with kind permission of Elsevier Science, from Ref. [60]).

be bound (side view) to two or four external sulphur atoms. When the slab size increases, the relative proportion of each Mo type varies differently with, specifically for symmetrical model slabs, the presence of a maximum for Mo at edge position Mo(e). The amount of chemisorbed O_2 and curves reporting variations of catalytic activity when the Mo loading on the support increases, closely resembles the variation of Mo(e)/Mo(total). This is a strong indication that the rate limiting step for the studied reactions as well as for O_2 adsorption occur at the edges of the MoS_2 platelets.

In addition to this model, experimental evidences [61,62] have shown that the supported MoS_2 phase has, after the sulphidation stage, and by reference to the stoichiometry S/Mo=2/1, an excess of sulphur (S/Mo=2.36) like in the models shown in Fig. 12 with complete saturation of sulphur around the slab (S/Mo=2.46 for a hexagonal slab containing 61 Mo atoms). Interactions with flowing hydrogen, starting from room temperature, permits to progressively remove excess of sulphur (S/Mo=1.96 after treatment at 473 K) or even to decrease the stoichiometry far below 2 (S/Mo=1.30 after treatment at 973 K). Such evolutions, which do not destroy the core of the MoS_2 crystallites for treatments lower than ~1000 K, correspond to removal of peripheral sulphur and creation of coordinative unsaturated sites (CUS). On the freshly sulphided catalysts, when no CUS is present, hydrogenation of unsaturated hydrocarbons is not detected but as long as the CUS are created, probe dienes are hydrogenated and isomerized [61–64] which permits to conclude that these reactions occur at such unsaturations. Further modelling of the CUS structure, i.e.location at the edge of MoS_2 and number of sulphur vacancy, has demonstrated the role of an ensemble site associating two adjacent Mo atoms at the edges of type (II) of Fig. 12[65]. More generally, CUS should play a major role in numerous hydroprocessing reactions but other sites, like SH groups at proximity of CUS, may have also an important role. Nevertheless, the recent investigations by Knözinger and coworkers [66] have really confirmed the existence of CUS at edges of MoS_2.

We focused the previous discussion on single layered MoS_2 slabs. In the "Rim-Edge" model of Daage and Chianelli [67], the role of MoS_2 stacking (Fig. 13) has been emphasized during reaction with dibenzothiophene (DBT). The top and bottom MoS_2 layers of the crystallites are associated with rim sites whereas the inner layers of the crystallites are associated with edge sites. It has been found that the hydrogenation reaction occurs exclusively on the rim sites whereas sulphur hydrogenolysis (in biphenyl formation, see Fig. 1(b)) is obtained on both rim and edge sites. Such an easy differentiation mainly occurs because of steric hindrance around the exposed site by adsorbed DBT.

4.2. *Role of promoters*

Part B of Fig. 11 has already shown the role of promoters (Co or Ni in conventional catalysts): MoS_2 by itself is moderately active in all the reactions involved during hydroprocessing but the addition of controlled amounts of promoter greatly enhances the catalytic performances. On the other hand, particles of cobalt or nickel sulphides (Co_9S_8, Ni_3S_2) when alone on the support are not active. Exceptions can be found in some cases, as already mentioned [58], when small crystallites of promoter sulphide may exhibit interesting catalytic properties.

A large number of descriptions of the promotion effect and relevant theories have been published in the literature. In the present paper, we will restrict ourselves to some aspects which appear decisive. By

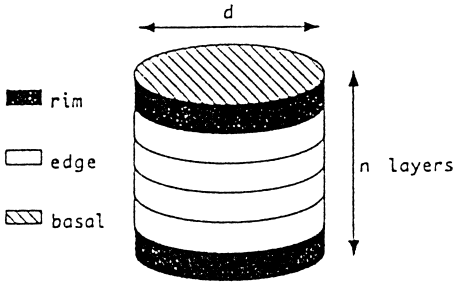

Fig. 13. Rim/Edge model of a MoS_2 catalyst particle (reproduced with kind permission of Academic Press from Ref. [67]).

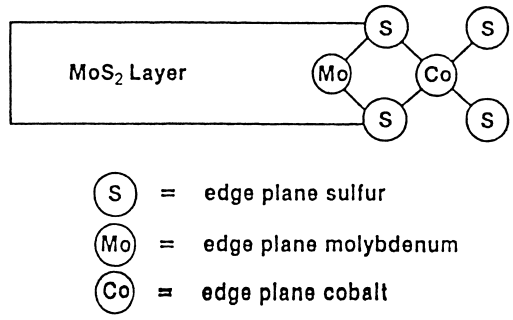

Fig. 14. Schematic representation of Co species interacting with the edges of MoS_2 (reproduced with kind permission of Academic Press, from Ref. [74]).

comparing a series of transition metal sulphides, Pecoraro and Chianelli [68] found correlations between metal–sulphur bond strength as deduced from thermodynamic heat of formation of the relevant sulphides and catalytic activity; the most active systems have intermediate values of the heat of formation and thus intermediate metal–sulphur bond strengths. Moreover, presence of 4d or 5d metals is necessary for high catalytic activity. It is therefore inferred that electronic factors are also crucial for developing highly active systems.

By performing calculations on MS_6^{n-} clusters, Harris and Chianelli [69] defined an activity parameter which takes into account different electronic factors; they are the number of electrons in the highest occupied orbital, the degree of covalency in the metal–sulphur bond and the covalent contribution to the metal–sulphur covalent bond strength. Further calculations [70] on $MoM'S_9^{n-}$ clusters (M′ being a 3d transition metal) indicate that the dominant electronic factor related to promotion of MoS_2 is the increase of "d" electrons associated with Mo. As a matter of fact, in the presence of Co or Ni, Mo is reduced relative to the Mo present in pure MoS_2. On the other hand, in the presence of Cu, Mo is formally oxidized: Cu is known as being a poison of MoS_2 rather than a promoter. XPS data have indeed confirmed that Co or Ni in promoted Co–MoS_2 or Ni–MoS_2 systems are electron donating species [71,72]. A detailed description of all the electronic effects in transition metal sulphide catalysts has been reviewed by Harris and Chianelli [73].

Such electron donating properties of efficient promoters of MoS_2 imply a real contact between Co(Ni) and MoS_2 like in the "Co–Mo–S" phase identified by MES and schematically represented in Fig. 14 [79].

More precise location and environment of the promoter in the Co–Mo–S phase has been described and discussed by Topsøe et al. [75], mainly from EXAFS data. Co is located in the same plane of Mo atoms in MoS_2 at the edges of the crystallites with a Co–Mo distance of 2.8 Å, a value smaller than the Mo–Mo distance in MoS_2 (3.16 Å). Co edge atoms could be located in distorted pyramidal or trigonal prismatic coordination. NMR results are more in favour of the existence of an octahedral cobalt species [76].

Nevertheless, whatever the precise environment around the cobalt species "decorating" the MoS_2 edges, the relevant question is relative to the nature of active sites concerned by promoted MoS_2. Does the promoter enhance the catalytic activity, probably by electron transfer, of the Mo edge site or does it provide new sites? The new site could be anionic vacancies shared by Co and Mo (mixed site) or localized only on Co(Ni). In this latter case, the catalyst description would be that MoS_2 is a support for well dispersed active Co or Ni species, all the system being supported on alumina. Further studies are needed to clarify these questions. However, adsorption of probe molecules already enlighted some aspects; i.e. the IR lines of NO adsorbed on CUS of free MoS_2 edges ($17\,801\,685\ cm^{-1}$) are shifted to $18\,501\,785\ cm^{-1}$ on Co–MoS_2 and correspond to adsorption on promoted sites [77]. The intensity of the latter is correlated with catalytic activity.

Another important description of the promoting role of Co(Ni) in hydrotreating reactions comes from the works of Delmon [78,81] who proposes that synergy occurs through remote control of one phase (or spe-

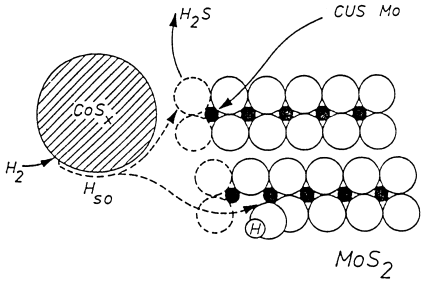

Fig. 15. Schematic representation of the formation of CUS at MoS_2 by action of H species created on the Co sulphide particles (reproduced with kind permission of World Scientific Publishing Co., from Ref. [80]).

cies) over another one and that the hydrogen species are spilled over the support. Fig. 15 illustrates the proposals of Delmon. The particles of cobalt sulphide adsorb and dissociate hydrogen. The H species are mobile enough in the conditions of catalysis to attack the MoS_2 particles and create coordinative unsaturations at the edges. The active sites are then operating in the diverse reactions to proceed. The remote control mechanism appears general in HDT catalysis and influences activity and selectivity patterns for selected reactions. It has also been evidenced when mechanical mixtures of different solids are used.

The above theories concerning the promotion of MoS_2 patches are different but the preparation of the samples appears quite important for their respective influence. For example, the presence of very small crystallites of either Co or Mo sulphides, not detected by HREM, or even the presence of individual species may considerably affect the catalytic behaviours.

4.3. Mechanistic aspects

Since hydroprocessing reactions are studied, numerous papers try to get informations on the kinetic aspects and products distribution in order to establish the mechanism of molecules transformation at the surface of the catalysts. For example, Perot [3] in his review article considered in detail the mechanisms of HDN of representative molecules. In this paragraph, we wish only to focus attention on HDS reactions. In an excellent review, Angelici [82] discussed very precisely the different modes of interaction of thiophenic molecules with metal centres by reference to organometallic complexes which can be considered, for some of them, as the active sites with surrounding ligands at the surface of practical catalysts. S atom directly bound to the metal or adsorption through the aromatic ring may both occur. Thiophene adsorbed to a metal site through all five atoms (η^5) [83–85] is activated and can be attacked by a surface hydride at the 2-position (Fig. 16, step (a)). Then, a strongly acidic H^+, the origin of which could be a SH group adjacent to the metal site, is added in the second step (b) to the 3-position, forming 2,3-dihydrothiophene which further isomerizes in 2-5 dihydrothiophene (step (c)). The next step (d) gives butadiene and S adsorbed. H_2 then removes S as H_2S and regenerates the active site (step (e)). This mechanism established from studies with organometallic compounds [83–85]

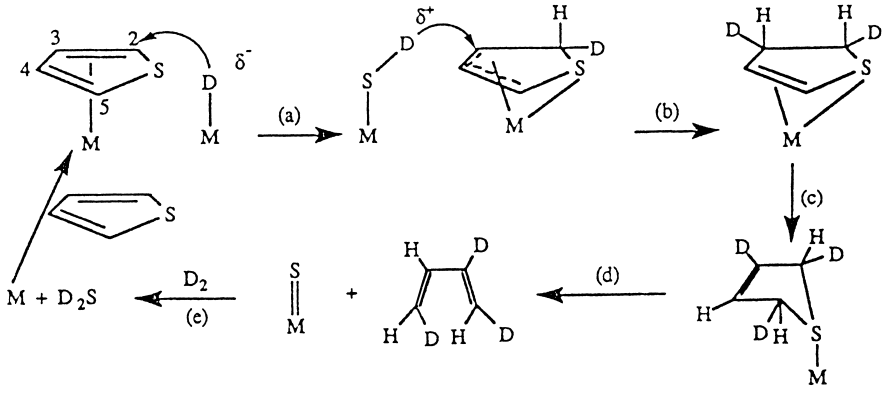

Fig. 16. Example of one possible mechanism proposed for HDS of thiophene. Deuterium (D) incorporation into butadiene is described (reproduced with kind permission of Elsevier Science, from Ref. [87]).

is interesting as it proposes two different attacks by hydrogen acting as H^- and H^+. This scheme can be correlated to the observations on MoS_2 of the presence of SH groups in addition to S unsaturations and also to the evidence of a H reservoir [86].

Very recently, Angelici et al. [87] critically compared the different mechanisms proposed in the literature, including the one reported in Fig. 16 from studies of deuterodesulphurization of thiophene. The verdict is that any mechanism that produce butadiene with more than 3.2 D are inconsistent with the experimental results.

5. Conclusion

The aim of this review is rather to be more comprehensive than exhaustive. The references are provided for those who want more detail. The current developments of hydrotreating catalysts are focused towards a better design either in the choice of the support, or in the preparation steps, or in the selection of ingredients (Mo, promoters, additives) or in the activation procedures. A good choice of these parameters should provide to the catalysts

higher activity,
better selectivity and even polyfunctionality,
acceptable resistance to sintering and poisoning,
easy and efficient regeneration.

For achieving some of these criteria, several solutions are studied, some will probably lead to a new generation of catalysts for the next century.

References

[1] F.E. Massoth, G. Muralidhar, in: H.F. Barry, P.C.H. Mitchell (Eds.), Proceedings of the Climax Fourth International Conference on the Chemistry and Uses of Molybdenum, Climax Molybdenum Company, Ann Arbor, 1982, p. 343.
[2] M.L. Vrinat, in: J.P. Bonnelle, B. Delmon, E. Derouane (Eds.), Surface Properties and Catalysis by Non-Metals , D. Reidel Publishing Company, 1983, p. 391, and references therein.
[3] G. Perot, Catal. Today 10 (1991) 447.
[4] F. Vandeneeckoute, R. Hubaut, S. Pietrzyk, T. Des Courieres, J. Grimblot, React. Kinet. Catal. Lett. 45 (1991) 191.
[5] R. Hubaut, S. Dejonghe, J. Grimblot, J.P. Bonnelle, React. Kinet. Catal. Lett. 51 (1993) 9.
[6] J.P. Brunelle, Pure Appl. Chem. 50 (1978) 1211.
[7] G.A. Tsigdinos, H.Y. Chen, B.J. Streusand, Ind. Eng. Chem., Prod. Res. Dev. 20 (1981) 619.
[8] L. Wang, W.K. Hall, J. Catal. 77 (1982) 232.
[9] S. Kasztelan, J. Grimblot, J.P. Bonnelle, E. Payen, H. Toulhoat, Y. Jacquin, Appl. Catal. 7 (1983) 91.
[10] N.P. Luthra, W.C. Cheng, J. Catal. 107 (1987) 154.
[11] P. Sarrazin, B. Mouchel, S. Kasztelan, J. Phys. Chem. 93 (1989) 904.
[12] P. Sarrazin, S. Kasztelan, E. Payen, J.P. Bonnelle, J. Gimblot, J. Phys. Chem. 97 (1993) 5954.
[13] H. Jeziorowski, H. Knözinger, J. Phys. Chem. 83 (1979) 1166.
[14] E. Payen, J. Barbillat, J. Grimblot, J.P. Bonnelle, Spectrosc. Lett. 11 (1978) 997.
[15] B. Sombret, P. Dhamelincourt, F. Wallart, A.C. Muller, M. Bouquet, J. Gromangin, J. Raman Spectrosc. 9 (1980) 291.
[16] D.S. Zing, L.E. Makowsky, R.E. Tisher, F.R. Brown, D.M. Hercules, J. Phys. Chem. 84 (1980) 2898.
[17] C.P. Cheng, G.L. Schrader, J. Catal. 60 (1979) 276.
[18] E. Payen, S. Kasztelan, J. Grimblot, J.P. Bonnelle, Polyhedron 5 (1986) 157.
[19] E. Payen, S. Kasztelan, J. Grimblot, J. Phys. Chem. 91 (1987) 6642.
[20] F.M. Mulcahy, M.J. Fay, A. Proctor, M. Houalla, D.M. Hercules, J. Catal. 124 (1990) 231.
[21] C.T.J. Mensch, J.A.R. Van Veen, B. Van Wingerden, M.P.J. Van Dijk, J. Phys. Chem. 92 (1988) 4961.
[22] J.A.R. Van Veen, P.A.J.M. Hendriks, E.J.G.M. Romers, R.R. Andrea, J. Phys. Chem. 94 (1990) 5275.
[23] J. Grimblot, J.P. Bonnelle, J.P. Beaufils, J. Electron Spectrosc. Related Phenom. 8 (1976) 437.
[24] P. Dufresne, E. Payen, J. Grimblot, J.P. Bonnelle, J. Phys. Chem. 85 (1981) 2344.
[25] J.L. Paulhiac, O. Clause, J. Am. Chem. Soc. 115 (1993) 11602.
[26] J.B. D'Espinose De La Caillerie, C. Bobin, B. Rebours, O. Clause, in: G. Poncelets et al. (Eds.), Preparation of Catalysts VI, Scientific Bases for the Preparation of Heterogeneous Catalysts, Elsevier, Amsterdam, 1995, p. 169.
[27] R. Mone, in: B. Delmon et al. (Eds.), Preparation of Catalysts, Elsevier, Amsterdam, 1976, 381.
[28] J. Abart, E. Delgado, G. Ertl, H. Jeziorowski, H. Knözinger, N. Thiele, X.Z. Wang, E. Taglauer, Appl. Catal. 2 (1982) 155.
[29] H. Jeziorowski, H. Knözinger, E. Taglauer, C. Vogdt, J. Catal. 80 (1983) 286.
[30] S. Kasztelan, J. Grimblot, J.P. Bonnelle, J. Phys. Chem. 91 (1987) 1503.
[31] N. Spanos, A. Lycourghiotis, Langmuir 9 (1993) 2250; 10 (1994) 2351.
[32] N. Spanos, A. Lycourghiotis, J. Colloid Interf. Sci. 171 (1995) 306.
[33] F. Mauge, J.C. Duchet, J.C. Lavalley, S. Houssenbay, E. Payen, J. Grimblot, S. Kasztelan, Catal. Today 10 (1991) 561.
[34] Y. Yoshmura, N. Matsubayashi, T. Sato, H. Shimada, A. Nishijima, Appl. Catal. 79 (1991) 145.

[35] J.A.R. Van Veen, E. Gerdema, A.M. Van der Kraan, A. Knoester, J. Chem. Soc., Chem. Comm. (1987) 1684.
[36] P. Blanchard, C. Mauchausse, E. Payen, J. Grimblot, O. Poulet, N. Boisdron, R. Loutaty, in: G. Poncelet et al. (Eds.), Preparation of Catalysts VI, Scientific Bases for the Preparation of Heterogeneous Catalysts, Elsevier, Amsterdam, 1995, p. 1037.
[37] E. Etienne, E. Ponthieu, E. Payen, J. Grimblot, J. Non-Cryst. Solids 147, 148 (1992) 764.
[38] L. Le Bihan, C. Mauchausse, L. Duhamel, J. Grimblot, E. Payen, J. Sol–Gel Sci. Technol. 2 (1994) 837.
[39] P. Arnoldy, J.A.M. Van Den Heijkant, G.D. De Bok, J.A. Moulijn, J. Catal. 92 (1985) 35.
[40] B. Scheffer, J.C.M. De Jonge, P. Arnoldy, J.A. Moulijn, Bull. Soc. Chim. Belg. 93 (1984).
[41] B. Scheffer, P. Arnoldy, J.A. Moulijn, J. Catal. 112 (1988) 516.
[42] E. Payen, S. Kasztelan, S. Houssenbay, R. Szymanski, J. Grimblot, J. Phys. Chem. 93 (1989) 6501.
[43] K.S. Liang, R.R. Chianelli, F.Z. Chien, S.C. Moss, J. Non-Cryst. Solids 79 (1986) 251.
[44] M.R. Hilton, P.D. Fleischauer, J. Mater. Res. 5 (1990) 406.
[45] E. Payen, R. Hubaut, S. Kasztelan, O. Poulet, J. Grimblot, J. Catal. 147 (1994) 123.
[46] S. Eijsbouts, J.J.L. Heinerman, H.J.W. Elzerman, Appl. Catal. A 105 (1993) 53.
[47] S. Eijsbouts, J.J.L. Heinerman, H.J.W. Elzerman, Appl. Catal. A 105 (1993) 69.
[48] S. Eijsbouts, G.C. Van Leerdam, Bull. Soc. Chim. Belg. 104 (1995) 347.
[49] H. Topsøe, B.S. Clausen, R. Candia, C. Wivel, S. Mørup, J. Catal. 68 (1981) 433.
[50] C. Wivel, R. Candia, B.S. Clausen, S. Mørup, H. Topsøe, J. Catal. 68 (1981) 453.
[51] H. Topsøe, B.S. Clausen, R. Candia, C. Wivel, S. Mørup, Bull. Soc. Chim. Belg. 90 (1981) 1190.
[52] H. Topsøe, R. Candia, N.Y. Topsøe, B.S. Clausen, Bull. Soc. Chim. Belg. 93 (1984) 783.
[53] H. Topsøe, B.S. Clausen, in: H. Heinemann, G. Somorjai (Eds.), Catalysis and Surface Science, Dekker, New York, 1985, p. 95.
[54] M.W.J. Craje, V.H.J. De Beer, A.M. Van Der Kraan, Hyp. Int. 69 (1991) 795.
[55] M.W.J. Craje, V.H.J. De Beer, A.M. Van Der Kraan, Appl. Catal. 70 (1991) L7.
[56] M.W.J. Craje, S.P.A. Louwers, V.H.J. De Beer, R. Prins, A.M. Van Der Kraan, J. Phys. Chem. 96 (1992) 5445.
[57] M.W.J. Craje, V.H.J. De Beer, A.M. Van Der Kraan, Bull. Soc. Chim. Belg. 100 (1991) 953.
[58] J.P.R. Vissers, V.H.J. De Beer, R. Prins, J. Chem. Soc., Faraday Trans. I 83 (1987) 2145.
[59] R.R. Chianelli, A.F. Ruppert, S.K. Behal, B.H. Kear, A. Wold, R. Kershaw, J. Catal. 92 (1985) 56.
[60] S. Kasztelan, H. Toulhoat, J. Grimblot, J.P. Bonnelle, Appl. Catal. 13 (1984) 127.
[61] S. Kasztelan, L. Jalowiecki, A. Wambeke, J. Grimblot, J.P. Bonnelle, Bull. Soc. Chim. Belg. 96 (1987) 1003.
[62] A. Wambeke, L. Jalowiecki, S. Kasztelan, J. Grimblot, J.P. Bonnelle, J. Catal. 109 (1988) 320.
[63] R. Hubaut, O. Poulet, S. Kasztelan, J. Grimblot, J. Mol. Catal. 81 (1993) 301.
[64] S. Kasztelan, A. Wambeke, L. Jalowiecki, J. Grimblot, J.P. Bonnelle, J. Catal. 124 (1990) 12.
[65] L. Jalowiecki-Duhamel, J. Grimblot, J.P. Bonnelle, J. Catal. 129 (1991) 511.
[66] P. Mottner, T. Butz, A. Lerf, G. Ledezma, H. Knözinger, J. Phys. Chem. 99 (1995) 8260.
[67] M. Daage, R.R. Chianelli, J. Catal. 149 (1994) 414.
[68] T.A. Pecoraro, R.R. Chianelli, J. Catal. 67 (1981) 430.
[69] S. Harris, R.R. Chianelli, J. Catal. 86 (1984) 400.
[70] S. Harris, R.R. Chianelli, J. Catal. 98 (1986) 17.
[71] I. Alstrup, I. Chorkendorf, I. Candia, B.S. Clausen, H. Topsøe, J. Catal. 77 (1982) 397.
[72] S. Houssenbay, S. Kasztelan, H. Toulhoat, J.P. Bonnelle, J. Grimblot, J. Phys. Chem. 93 (1989) 7176.
[73] S. Harris, R.R. Chianelli, in: J.B. Moffat (Ed.), Theoretical Aspects of Heterogeneous Catalysis, Van Nostrand Reinhold, New York, 1990, p. 206.
[74] R.R. Chianelli, T.A. Pecoraro, T.R. Halbert, W. Pan, E.I. Stiefel, J. Catal. 86 (1984) 226.
[75] H. Topsøe, B.S. Clausen, N.Y. Topsøe, P. Zeuthen, in: D.L. Trimm et al. (Eds.), Catalysts in Petroleum Refining 1989, Elsevier, Amsterdam, 1990, p. 77 and references therein.
[76] M.J. Ledoux, O. Michaux, G. Agostini, P. Panissod, J. Catal. 96 (1985) 189.
[77] N.Y. Topsøe, H. Topsøe, J. Catal. 84 (1983) 386.
[78] B. Delmon, in: D.L. Trimm et al. (Eds.), Catalysts in Petroleum Refining 1989, Elsevier, Amsterdam, 1990, p. 1.
[79] B. Delmon, Catal. Lett. 22 (1993) 1.
[80] B. Delmon, Surf. Rev. Lett. 2 (1995) 25.
[81] B. Delmon, Bull. Soc. Chim. Belg. 95 (1995) 173.
[82] R.J. Angelici, Bull. Soc. Chim. Belg. 95 (1995) 265.
[83] R.J. Angelici, Acc. Chem. Res. 22 (1988) 387.
[84] N.N. Sauer, E.J. Markel, G.L. Schrader, R.J. Angelici, J. Catal. 117 (1989) 295.
[85] E.J. Markel, G.L. Schrader, N.N. Sauer, R.J. Angelici, J. Catal. 116 (1989) 11.
[86] L. Jalowiecki, J. Grimblot, J.P. Bonnelle, J. Catal. 126 (1990) 101.
[87] J.W. Benson, G.L. Schrader, R.J. Angelici, J. Mol. Catal. A, Chem. 96 (1995) 283.